Research Square

Preprints are preliminary reports that have not undergone peer review.
They should not be considered conclusive, used to inform clinical practice,
or referenced by the media as validated information.

Hyperchloremic Acidosis Alters the Kinetic Properties of Transport ATPases in the Rat Hippocampus

Nikoloz Zhgenti

nikoloz.zhgenti@tsu.ge

Tbilisi State University

Otar Bibilashvili

Tbilisi State University

Nana Koshoridze

Tbilisi State University

Marine Koshoridze

Tbilisi State University

Elene Davitashvili

Tbilisi State University

Research Article

Keywords: Hyperchloremic acidosis, Metabolic acidosis, Na/K-ATPase, Ca-ATPase, Anion-ATPases

Posted Date: October 21st, 2026

DOI: https://doi.org/10.21203/rs.3.rs-10973142/v1

License: This work is licensed under a Creative Commons Attribution 4.0 International License.
Read Full License

Additional Declarations: No competing interests reported.

Abstract

Hyperchloremic acidosis is a common acid–base disturbance, yet its effects on membrane transport ATPases in the hippocampus remain poorly characterized. This study investigated the activity and kinetic properties of Na^+/K^+-, Ca^{2+}-, and HCO_3^--ATPases in the hippocampus of rats with experimentally induced hyperchloremic acidosis. Hyperchloremic acidosis was confirmed by reduced plasma pH and HCO_3^- concentration and increased Cl^- concentration, without significant changes in Na^+ or K^+. The activities of Na^+/K^+-ATPase, Ca^{2+}-ATPase, and Mg^{2+}-dependent HCO_3^--ATPase were significantly reduced, whereas Mg^{2+}-independent HCO_3^--ATPase activity was increased. Isoform analysis revealed greater suppression of the α1 than α2/3 Na^+/K^+-ATPase fraction. Kinetic analysis demonstrated reduced Vmax of Na^+/K^+-, Ca^{2+}-, and Mg^{2+}-dependent HCO_3^--ATPases without significant changes in substrate Km, except for K^+, for which Km increased. Conversely, Mg^{2+}-independent HCO_3^--ATPase showed increased Vmax with unchanged Km. These findings demonstrate that hyperchloremic acidosis differentially modifies hippocampal transport ATPases, affecting their catalytic capacity and, selectively, substrate affinity. Such alterations may contribute to disruption of ionic and acid–base homeostasis in the hippocampus during systemic acidosis.

1. Introduction

Hyperchloremic acidosis is a form of metabolic acidosis characterized by a reduction in plasma bicarbonate concentration accompanied by an elevation of plasma chloride, occurring without a corresponding increase in the anion gap (Bhandari et al. 2024; Palmer and Clegg 2019). In clinical practice it arises most commonly from excessive gastrointestinal bicarbonate loss (severe diarrhea), renal tubular acidosis, and, increasingly, from large-volume resuscitation with 0.9% saline, which supplies chloride in excess of plasma levels and dilutes endogenous bicarbonate and protein buffers (Kraut and Kurtz 2014; Palmer and Clegg 2019; Haines et al. 2019). Experimentally, chronic hyperchloremic metabolic acidosis can be reliably induced by administration of ammonium chloride (NH_4Cl), commonly provided in the drinking water of rodents. NH_4Cl loading imposes a systemic acid burden and stimulates renal mechanisms involved in acid excretion and ammonium handling, resulting in reduced blood pH and bicarbonate concentrations accompanied by increased chloride concentrations. This model has been extensively used to reproduce sustained metabolic acidosis in experimental animals and to investigate its renal and systemic consequences (Kwon et al. 2001; Nowik et al 2011; Johnsen et al. 2024). Understanding the consequences of this acid-base disturbance for the central nervous system is important because the brain, and the hippocampus in particular, is highly sensitive to shifts in extracellular and intracellular pH: acidosis alters neuronal excitability, ion channel gating, synaptic transmission, and, as central chemoreceptors on the ventral brainstem respond to interstitial pH, ventilatory drive itself (Ruffin et al. 2014; Hsu et al. 2000; Guyenet and Bayliss 2022).

Transport ATPases are of particular interest in this context because they are central to the establishment and maintenance of the ionic gradients that underlie neuronal signaling, membrane excitability, cell-volume regulation, and intracellular pH homeostasis. These processes depend heavily on ATP-driven ion

pumps, including Na^+/K^+-ATPase and Ca^{2+}-ATPases, which directly couple ATP hydrolysis to the transport of ions against their electrochemical gradients (Blaustein et al. 2020; Dyla et al. 2020; Shrivastava et al. 2018). In the brain, this energetic demand is particularly substantial because restoration of ionic gradients following neuronal activity represents a major component of cellular energy expenditure, with Na^+/K^+-ATPase activity accounting for a substantial fraction of the brain's ATP utilization (de Lores Arnaiz and Ordieres 2014). At the same time, neuronal and glial pH homeostasis is tightly coupled to transmembrane ion transport, including Na^+/H^+ exchange, Na^+-dependent Cl^-/HCO_3^- exchange, and Na^+/HCO_3^- cotransport (Sengupta et al. 2010). Because systemic acid-base disturbances can alter extracellular and intracellular pH and thereby modify ion transport, channel activity, and intracellular Ca^{2+} handling, ATP-dependent transport systems represent plausible molecular targets through which metabolic acidosis may influence cerebral ion homeostasis and neuronal function (Chesler 2003; Gerkau et al. 2019).

The Na^+/K^+-ATPase is the principal ATP-dependent mechanism responsible for maintaining the transmembrane Na^+ and K^+ gradients that underlie the neuronal resting membrane potential and accounts for a substantial fraction of neuronal and brain energy consumption (Shrivastava et al. 2018; Berndt and Holzhütter 2013). It belongs to the P-type ATPase superfamily and consists primarily of a catalytic α-subunit containing 10 transmembrane helices and three major cytoplasmic domains, the nucleotide-binding (N), phosphorylation (P), and actuator (A) domains, that coordinate the phosphorylation and dephosphorylation of a conserved aspartate residue during the Post-Albers catalytic cycle (Nielsen et al. 2024; Ivanov et al. 2000). The α-subunit associates with a heavily glycosylated β-subunit that is important for proper membrane assembly and functional maturation, while FXYD-family proteins serve as tissue- and isoform-dependent regulatory partners that modulate pump kinetics and ion affinity (Meyer et al. 2020). In the brain, the α1 and α3 Na^+/K^+-ATPase isoforms are widely expressed in neurons, whereas α2 is enriched predominantly in astrocytes, although isoform expression can overlap among neuronal and glial populations (Holm and Lykke-Hartmann 2016). The distinct kinetic properties and cellular distribution of these isoforms suggest that their contribution to ion homeostasis may vary according to cell type and physiological state. In the NH_4Cl-induced acidosis model, preservation of circulating Na^+ and K^+ concentrations would minimize changes in extracellular substrate availability for the Na^+/K^+-ATPase; consequently, alterations in pump kinetics may instead reflect effects of the acid-base disturbance on enzyme conformation, protonation state, regulatory mechanisms, or the intracellular ionic environment. However, this interpretation should be considered mechanistically plausible rather than inferred solely from unchanged plasma Na^+ and K^+ concentrations (Lina and Kuijpers 2004).

Mg^{2+}-dependent Ca^{2+}-ATPase activity in brain membrane preparations is attributed predominantly to plasma membrane Ca^{2+}-ATPases (PMCAs), which are high-affinity Ca^{2+} pumps responsible for extruding cytosolic Ca^{2+} across the plasma membrane and thereby maintaining the low intracellular Ca^{2+} concentration required for neuronal signaling and survival (Strehler et al. 2007; Peggion et al. 2025). PMCA belongs to the P-type ATPase superfamily and utilizes MgATP in its catalytic cycle, forming a transient phosphorylated intermediate during Ca^{2+} transport. PMCA activity is regulated by a C-terminal

autoinhibitory domain containing a calmodulin-binding region; binding of Ca^{2+}-calmodulin relieves this autoinhibition and markedly increases pump activity and Ca^{2+} affinity (Brini and Carafoli 2011). Four PMCA gene products (PMCA1-4) are expressed in the mammalian brain, with PMCA2 and PMCA3 showing prominent expression in the central nervous system, although the individual isoforms exhibit distinct regional and cellular distributions (Slaughter et al. 2007; Domi et al. 2007; Boczek et al. 2019). Because PMCA-mediated Ca^{2+} extrusion is coupled to proton movement and is sensitive to the cellular acid-base environment, PMCA represents a potentially important link between intracellular pH regulation and neuronal Ca^{2+} homeostasis (Boczek et al. 2014).

Finally, brain membranes exhibit anion-stimulated ATPase activities that differ in their dependence on Mg^{2+}. A Mg^{2+}-dependent Cl^-/HCO_3^--stimulated ATPase activity has been identified in neuronal membranes and associated with the intracellular domains of GABA(A) receptor β-subunits. Experimental evidence indicates that β1- and β3-containing receptor complexes can exhibit Cl^--stimulated ATPase activity, whereas β3 is particularly associated with combined Cl^-/HCO_3^--ATPase activity and ATP-dependent regulation of anion transport (Menzikov et al. 2021; Menzikov et al. 2022; Menzikov et al. 2023). HCO_3^- can substantially enhance and stabilize this ATPase activity, suggesting a functional relationship between GABA(A) receptor signaling and neuronal Cl^-/HCO_3^- homeostasis. In parallel, a distinct Mg^{2+}-independent HCO_3^--stimulated ATPase has been characterized in synaptosomal and microsomal fractions of rat brain, demonstrating kinetic properties distinct from those of the Mg^{2+}-dependent enzyme (Dzneladze et al. 2015). Because these ATPase activities are directly regulated by Cl^- and/or HCO_3^-, alterations in extracellular and intracellular acid-base conditions may influence their activity and kinetic properties. Thus, these systems provide a plausible molecular link between hyperchloremic acidosis and altered neuronal anion homeostasis, warranting investigation of their kinetic behavior in the hippocampus.

2. Materials and Methods

2.1 Study Design

The research was conducted on 30 Lewis male laboratory rats, weighing 250 ± 25 g. Animals were housed and maintained in accordance with the Guide for the Care and Use of Laboratory Animals (2011) at the Department of Biology, Iv. Javakhishvili Tbilisi State University. All experimental procedures were approved by the institutional ethics committee and performed in accordance with the ARRIVE guidelines (Animal Research: Reporting of In Vivo Experiments) (Percie du Sert et al. 2020). Throughout the study, the rats had unrestricted access to both water and standard laboratory-grade food. The ambient room temperature was rigorously maintained at 22 ± 2∘C to ensure a stable and comfortable environment for the animals. Furthermore, the rats were subjected to a controlled 12-hour light-dark cycle to mimic their natural circadian rhythm.

Before the commencement of any experimental procedures, the rats were allowed a period of 7 days for acclimatization to the vivarium conditions. Following this adaptation phase, they were randomly divided

into two distinct experimental groups, each composed of 15 rats:

- Group I (Control): Rats received standard laboratory-grade food and drinking water *ad libitum*
- Group II (Hyperchloremic Acidosis model): Rats received standard laboratory-grade food and 0.28M ammonium chloride (NH_4Cl) in drinking water *ad libitum*, for 14 days.

On the 14th day of the study, the animals from each group were euthanized according to international guidelines (AVMA 2020). After euthanizing the animals, we decapitated them. The blood was collected from tail vein and plasma was separated as described earlier (Abatan et al. 2008). Then brains were removed. Using the rodent brain coronal matrice (RBMS-300C), stereomicroscope (Laxco LMS-Z230PMZS33) and rat brain atlas, we dissected the hippocampus and froze at -80 ◦C.

2.2 Model Validation

For validation of hyperchloremic acidosis pH, $HCO3^-$, Cl^-, Na^+, and K^+ levels were studied in blood plasma using comertial assay kits (ab228552, Z01MM-0326-JL1258, MAK510-1KT, ab211096, NBP3-25780).

2.3 Subcellular Fractionation

Fractionation of brain tissue was performed as as per Whittaker (1969). Briefly, rat hippocampus tissues were homogenized in 0.32 M sucrose and centrifuged at 1,000× g for 10 min. The supernatant (S1) was collected and centrifuged at 17,000× g for 55 min, resulting in the S2 supernatant and the P2 pellet (crude mitochondrial fraction). S2 was centrifuged at 100,000× g for one hour to generate the supernatant (cytosol fraction). P2 was resuspended in 0.32 M sucrose and layered onto a 1.2 M, 0.8 M block sucrose gradient. Following centrifugation at 53,000× g for two hours, fractions A (0.32/0.8M boundary), B (0.8/1.2 M boundary), and C (pellet below 1.2 M) (pure mitochondrial fraction) were collected and centrifuged at 100,000× g for one hour to isolate membranes. Pure mitochondrial and cytosol fractions were used for further experiments (Zhgenti et al. 2025a, b).

2.4 Na/K ATPase activity and Kinetic Properties

The samples were incubated for 15 min at 37°C. The difference between these two assays was used to compute the activity from Na/K ATPase. The amount of inorganic phosphate (Pi) produced by enzyme-induced ATP hydrolysis was used to calculate ATPase activity (per mg protein and per hour). Na/K-ATPase activity was expressed as μmol Pi/mg protein per hour (Chkadua et al. 2024). In rodents, the Na/K-ATPase α1 isoform is 1000 times less sensitive to the cardiac glycoside ouabain than the Na/K ATPase α2/3 isoforms, thereby allowing the α2/3-isoform fraction and α1 subunit activity to be evaluated independently with 3 μM and 3 mM ouabain (Kinoshita et al. 2014). A colorimetric analysis of inorganic phosphate was thereafter performed (Fiske and Subbarow 1925; Chkadua et al. 2022).

2.5 Mg^{2+}-dependent Ca^{2+}-ATPase activity and Kinetic Properties

Mg^{2+}-dependent Ca^{2+}-ATPase activity was determined by measuring the amount of inorganic phosphate (Pi) released during ATP hydrolysis. The assay was performed in the presence of Mg^{2+} and different concentrations of Ca^{2+}, with ATP serving as the substrate. Following incubation under standardized conditions, the reaction was terminated and liberated Pi was quantified colorimetrically using the Fiske–Subbarow method. ATPase activity was expressed as μmol Pi released per mg protein per min. The dependence of enzyme activity on Ca^{2+} concentration was used to characterize the kinetic properties of Ca^{2+}-ATPase (Nozadze et al. 2015).

2.6 Mg^{2+}-dependent and Mg^{2+}-independent HCO_3^- -ATPase activity and Kinetic Properties

HCO_3^--ATPase activity. Mg^{2+}-dependent and Mg^{2+}-independent HCO_3^--ATPase activities were determined in membrane preparations by measuring ATP hydrolysis and quantifying the released inorganic phosphate (Pi). Mg^{2+}-dependent HCO_3^--ATPase activity was measured in the presence of Mg^{2+} and HCO_3^-, whereas Mg^{2+}-independent activity was determined in the absence of Mg^{2+}. The reaction was initiated by addition of ATP and terminated after a defined incubation period, followed by colorimetric determination of liberated Pi. Enzyme activity was expressed as μmol Pi·mg $protein^{-1}$·min^{-1}. For kinetic characterization, enzyme activity was determined at different concentrations of HCO_3^-, and kinetic parameters were calculated from the corresponding substrate-dependence curves (Dzneladze et al. 2015; Koshoridze et al. 2012).

2.7 Chemicals and Reagents

All the reagents were purchased from Sigma–Aldrich (Sigma–Aldrich Inc., St. Louis, USA) unless otherwise specified.

2.8 Statistical Analysis

All data are presented as mean ± SEM. Statistical analyses were performed using GraphPad Prism 9.0 (GraphPad Software, USA). Data distribution was assessed using the Shapiro–Wilk test. Comparisons between the control and social isolation groups were performed using an unpaired two-tailed Student's t-test. Where the data did not meet the assumptions of parametric analysis, the Mann–Whitney U test was used. A p value < 0.05 was considered statistically significant.

A kinetic analysis method of multi-sited enzyme systems was subsequently used to assess experimental curves. The "method of power function transformation" was used to determine the number of sites designated for the essential activators (n) (Chkadua et al. 2022a, b; Kometiani et al. 2007)

3. Results

3.1 Model Validation

Before investigating the transport ATPases, the experimental model was first validated by assessing selected plasma parameters. As shown in Fig. 1A, plasma pH was significantly reduced in mice with hyperchloremic acidosis (group II; $p < 0.001$). Plasma HCO_3^- concentration was also significantly decreased ($p < 0.01$), whereas Cl^- concentration was significantly increased ($p < 0.001$). In contrast, plasma Na^+ and K^+ concentrations did not differ significantly between the groups ($p > 0.05$) (Fig. 1B).

3.2 Activity of transport ATPases

In the next stage of the study, the activities of selected transport ATPases were assessed in plasmatic membrane of hippocampus of experimental animals. As shown in Fig. 2, the activities of Na^+/K^+-ATPase ($p < 0.001$), Ca^{2+}-ATPase ($p < 0.001$), and Mg^{2+}-dependent HCO_3^--ATPase ($p < 0.01$) were significantly reduced in animals with hyperchloremic acidosis (group II). In contrast, the activity of Mg^{2+}-independent HCO_3^--ATPase was significantly increased under hyperchloremic acidosis ($p < 0.001$).

3.3 Kinetic Properties of Na/K ATPase

After determining the total Na^+/K^+-ATPase activity, the activities of the α1 and α2/3 isoforms were assessed separately in hippocampus of experimental rats. In rodents, the Na^+/K^+-ATPase α1 isoform is approximately 1,000-fold less sensitive to ouabain than the α2/3 isoforms, allowing the α2/3 fraction and α1 isoform activity to be evaluated independently using 3 μM and 3 mM ouabain, respectively. As shown in Fig. 3, the activity of the α1 isoform was significantly reduced by 64% in animals with hyperchloremic acidosis ($p < 0.001$), whereas α2/3 isoform activity was reduced by only 32% ($p < 0.01$).

Na^+-dependent kinetic analysis of Na^+/K^+-ATPase activity demonstrated that hyperchloremic acidosis significantly decreased Vmax ($p < 0.01$), while Km for Na^+ remained unchanged (Fig. 4).

In contrast, K^+-dependent kinetic analysis revealed a significant increase in Km for K^+ ($p < 0.05$), accompanied by a decrease in Vmax ($p < 0.01$) (Fig. 5). These findings indicate a reduction in the maximal catalytic capacity of Na^+/K^+-ATPase and a decreased apparent affinity for K^+ under conditions of hyperchloremic acidosis.

3.4 Kinetic Properties of Mg^{2+}-dependent Ca^{2+}-ATPase

In the next stage of the study, the dependence of Mg^{2+}-dependent Ca^{2+}-ATPase activity on Ca^{2+} concentration was assessed. Kinetic analysis showed that hyperchloremic acidosis significantly reduced the Vmax of Mg^{2+}-dependent Ca^{2+}-ATPase in the rat hippocampus ($p < 0.001$), whereas Km for Ca^{2+} remained unchanged (Fig. 6).

3.5 Kinetic Properties of Mg^{2+}-dependent and Mg2+-independent HCO_3^- -ATPase

The kinetic characteristics of the anionic HCO_3^--ATPases were investigated in parallel with those of the cation-transporting ATPases, given the central role of HCO_3^- homeostasis in hyperchloremic acidosis. Two forms of HCO_3^--ATPase have been described: Mg^{2+}-dependent and Mg^{2+}-independent HCO_3^--ATPases, the latter being considered an ecto-ATPase [37]. As shown in Fig. 7, hyperchloremic acidosis significantly reduced the Vmax of the Mg^{2+}-dependent HCO_3^--ATPase ($p < 0.01$), whereas Km remained unchanged.

In contrast, both the overall activity (Fig. 2) and Vmax (Fig. 8) of the Mg^{2+}-independent HCO_3^--ATPase were significantly increased under hyperchloremic acidosis ($p < 0.001$), while Km remained unchanged.

4. Discussion

The present findings indicate that hyperchloremic acidosis is accompanied by a selective remodeling of membrane ATPase function rather than a uniform suppression of ATP-dependent transport. The most informative aspect of the data is that changes in enzyme capacity and substrate handling were not identical among the transport systems examined. This distinction is important because neuronal ion homeostasis depends on several energetically coupled transport processes whose relative contribution changes with cellular and extracellular conditions.

The Na^+/K^+-ATPase appears particularly vulnerable to the acid-base disturbance. This is of considerable physiological significance because maintenance of the transmembrane Na^+ and K^+ gradients represents a major energetic demand of the brain, with Na^+/K^+-ATPase activity accounting for a substantial fraction of cerebral energy consumption (Larsen et al. 2016). Consequently, impairment of pump capacity during acidosis could create a mismatch between the energetic requirements of ionic homeostasis and the ability of the membrane to sustain these gradients. Importantly, the kinetic pattern observed here argues against a simple loss of Na^+ recognition by the enzyme. The preservation of apparent Na^+ affinity despite reduced maximal activity is more consistent with altered catalytic turnover, reduced functional enzyme availability, changes in membrane organization, or modification of regulatory mechanisms. Direct effects of pH on Na^+/K^+-ATPase function are also biologically plausible, as protonation can influence cation-binding sites and conformational transitions within the catalytic cycle (Cornelius et al. 2018). Thus, the present findings are compatible with an alteration of pump turnover or catalytic-state distribution rather than a generalized loss of Na^+ binding. The altered K^+ kinetics provide an additional layer to this interpretation. The simultaneous reduction in maximal activity and increase in apparent K^+ Km indicate that, in addition to reduced catalytic capacity, the apparent interaction of the pump with extracellular K^+ is altered by the acid-base disturbance. This pattern is compatible with perturbation of the conformational equilibria through which Na^+/K^+-ATPase alternates between Na^+- and K^+-dependent states. Because ion binding and conformational transitions are mechanistically coupled within the Post-Albers cycle, changes in the physicochemical environment could affect apparent K^+ affinity without necessarily causing nonspecific enzyme inhibition. The present data therefore favor selective modification of pump kinetics rather than a generalized loss of enzymatic function. The differential response of the α1 and α2/3 subunits is also potentially important. Na^+/K^+-ATPase isoforms are not

functionally interchangeable: their expression is cell-type dependent and their kinetic and regulatory properties differ. In the CNS, α2 is enriched in astrocytes, whereas α3 is predominantly neuronal, while α1 is broadly expressed in both neuronal and glial populations (Illarionova et al. 2014; Richards et al. 2007). These isoforms make distinct contributions to extracellular K^+ regulation and neuronal excitability. Therefore, the greater alteration associated with α1 in the present membrane preparation should not be interpreted as evidence of preferential neuronal dysfunction. Rather, it may reflect the broader cellular distribution of α1, differences in isoform-specific regulation, or changes in the relative contribution of neuronal and glial membranes to the preparation.

The reduction in Mg^{2+}-dependent Ca^{2+}-ATPase capacity provides a second indication that acid-base disturbance may compromise mechanisms responsible for maintaining intracellular Ca^{2+} homeostasis. This is potentially consequential in neural tissue because Ca^{2+} functions not only as an ionic determinant but also as a central intracellular signaling molecule, with neuronal survival and synaptic function depending on tightly controlled spatial and temporal Ca^{2+} gradients (Gu et al. 2025). Plasma-membrane and intracellular Ca^{2+}-ATPases cooperate with exchangers and channels to maintain this control. The unchanged apparent Ca^{2+} affinity observed in the present study suggests that the predominant alteration is a reduction in functional capacity rather than a major change in the apparent interaction of the enzyme with Ca^{2+}. Nevertheless, reduced maximal activity could compromise the capacity of neuronal membranes to restore cytosolic Ca^{2+} following periods of elevated intracellular Ca^{2+} (Brini and Carafoli 2011).

The HCO_3^--ATPase findings are particularly noteworthy because they demonstrate that hyperchloremic acidosis does not uniformly suppress ATP-dependent membrane transport. Brain membranes contain kinetically distinguishable Mg^{2+}-dependent and Mg^{2+}-independent HCO_3^--stimulated ATPase activities, which have been characterized in synaptosomal and microsomal fractions of rat brain (Dzneladze et al. 2015). Their opposite responses in the present study therefore suggest that the acid-base disturbance affects these enzymatic systems through distinct regulatory mechanisms rather than producing generalized impairment of membrane ATPase function. One possible interpretation is that suppression of the Mg^{2+}-dependent pathway and enhancement of the Mg^{2+}-independent pathway represent divergent responses to the altered acid-base and ionic environment. The increase in Mg^{2+}-independent activity could reflect compensatory regulation of membrane-associated bicarbonate handling, whereas the reduction in Mg^{2+}-dependent activity may indicate greater sensitivity of this enzyme system to the altered biochemical environment. However, because the present experiments did not directly assess membrane localization, intracellular pH, or the molecular identity of these ATPase activities, an adaptive interpretation remains provisional.

Taken together, the data support a model in which hyperchloremic acidosis selectively remodels the functional balance among membrane ATPases involved in Na^+, K^+, Ca^{2+}, and HCO_3^- handling rather than producing a generalized suppression of ATP-dependent transport. The kinetic patterns are particularly informative because they distinguish reductions in maximal catalytic capacity from changes in apparent substrate interaction. Na^+/K^+-ATPase and Mg^{2+}-dependent Ca^{2+}-ATPase primarily exhibited reduced

maximal activity without a corresponding loss of apparent substrate affinity, whereas K^+ dependence of Na^+/K^+-ATPase was additionally altered. In contrast, the Mg^{2+}-dependent and Mg^{2+}-independent HCO_3^--ATPase activities changed in opposite directions, further supporting the existence of system-specific responses to the acid-base disturbance. Such differential remodeling may be physiologically more relevant than the magnitude of change in any individual enzyme because neuronal ion homeostasis depends on coordinated operation of multiple transport systems. Future studies integrating enzyme kinetics with intracellular pH and Ca^{2+} measurements, cellular ATP availability, transporter abundance, and isoform-specific molecular analyses will be necessary to determine whether these changes represent compensatory adaptations or contribute directly to impaired neuronal function during sustained acidosis.

5. Conclusion

Hyperchloremic acidosis markedly alters the functional properties of hippocampal transport ATPases, with impaired Na^+/K^+- and Ca^{2+}-ATPase capacity and distinct kinetic alterations in K^+ handling. In contrast, Mg^{2+}-dependent and Mg^{2+}-independent HCO_3^--ATPases respond divergently, suggesting selective rather than generalized disruption of membrane transport. These findings identify transport ATPases as potential functional targets of acid–base disturbances in the hippocampus.

Declarations

Author Contributions

Nikoloz Zhgenti: Conceptualization, Methodology, Investigation, Data curation, Formal analysis, Writing – original draft, Writing – review and editing, Supervision, Project administration. Otar Bibilashvili: Methodology, Data curation, Formal analysis, Writing – review and editing. Nana Koshoridze: Supervision, Data curation, Writing – review and editing. Marine Koshoridze: Data curation, Formal analysis, Writing – review and editing. Elene Davitashvili: Data curation, Formal analysis, Writing – review and editing. All authors have read and approved the final version of the manuscript.

Ethical Approval

The protocol employed in the study was approved by the Institutional Animal Care and Ethical Committee of the Tbilisi State University

Funding

This research did not receive any specific grant from funding agencies in the public, commercial, or non-for-profit sectors.

Declaration of Competing Interest

The authors declare that they have no known competing financial interests or personal relationships that could have appeared to influence the work reported in this paper.

Data Availability

Data will be made available on request.

Declaration of Generative AI And AI-Assisted Technologies

During the preparation of this work the authors used ChatGPT in order to improve language and grammar. After using this tool/service, the authors reviewed and edited the content as needed and takes full responsibility for the content of the publication.

Acknowledgments

We sincerely thank Prof. Gvantsa Chkadua for her valuable consultation on the methodological and statistical aspects of this study.

References

1. Abatan OI, Welch KB, Nemzek JA (2008) Evaluation of saphenous venipuncture and modified tail-clip blood collection in mice. J Am Assoc Lab Anim Sci 47(3):8–15
2. American Veterinary Medical Association (2020) AVMA guidelines for the euthanasia of animals: 2020 edition. American Veterinary Medical Association, Schaumburg, IL
3. Berndt N, Holzhütter HG (2013) The high energy demand of neuronal cells caused by passive leak currents is not a waste of energy. Cell Biochem Biophys 67:527–535. https://doi.org/10.1007/s12013-013-9538-3
4. Bhandari R, Ekladious A, Javaid MM (2024) Demystifying normal-anion-gap metabolic acidosis: pathophysiology, aetiology, evaluation and diagnosis. Intern Med J 54:1056–1065. https://doi.org/10.1111/imj.16418
5. Blaustein MP, Lariccia V, Khananshvili D, Annunziato L, Verkhratsky A (2020) Multipurpose Na+ ions mediate excitation and cellular homeostasis: evolution of the concept of Na+ pumps and Na+/Ca2 + exchangers. Cell Calcium 87:102166. https://doi.org/10.1016/j.ceca.2020.102166
6. Boczek T, Lisek M, Ferenc B, Kowalski A, Stepinski D, Wiktorska M, Zylinska L (2014) Plasma membrane Ca2+-ATPase isoforms composition regulates cellular pH homeostasis in differentiating PC12 cells in a manner dependent on cytosolic Ca2 + elevations. PLoS ONE 9:e102352. https://doi.org/10.1371/journal.pone.0102352
7. Boczek T, Radzik T, Ferenc B, Zylinska L (2019) The puzzling role of neuron-specific PMCA isoforms in the aging process. Int J Mol Sci 20:6338. https://doi.org/10.3390/ijms20246338
8. Brini M, Carafoli E (2011) The plasma membrane Ca2 + ATPase and the plasma membrane sodium calcium exchanger cooperate in the regulation of cell calcium. Cold Spring Harb Perspect Biol

3:a004168. https://doi.org/10.1101/cshperspect.a004168

9. Chesler M (2003) Regulation and modulation of pH in the brain. Physiol Rev 83:1183–1221. https://doi.org/10.1152/physrev.00010.2003
10. Chkadua G, Nozadze E, Tsakadze L, Shioshvili L, Arutinova N, Leladze M, Dzneladze S (2015) Comparative analysis of Mg-dependent and Mg-independent HCO3 – ATPases. J Membr Biol 248:53–58. https://doi.org/10.1007/s00232-014-9739-8
11. Chkadua G, Nozadze E, Tsakadze L, Shioshvili L, Leladze M, Arutinova N, Dzneladze S, Javakhishvili M, Kupradze S (2022a) Effect of H2O2 on Na,K-ATPase. J Bioenerg Biomembr 54:241–249. https://doi.org/10.1007/s10863-022-09948-1
12. Chkadua G, Nozadze E, Tsakadze L, Shioshvili L, Leladze M, Arutinova N, Dzneladze S, Javakhishvili M, Kupradze S (2022b) Some kinetic features of Na,K-ATPase and sensitivity to noradrenaline. Cell Biochem Biophys 80:23–29. https://doi.org/10.1007/s12013-021-01032-6
13. Chkadua G, Nozadze E, Tsakadze L, Shioshvili L, Arutinova N, Leladze M, Dzneladze S, Javakhishvili M, Jariashvili T, Petriashvili E (2024) The effect of cytochrome c on Na,K-ATPase. J Bioenerg Biomembr 56:221–234. https://doi.org/10.1007/s10863-024-10012-3
14. Cornelius F, Tsunekawa N, Toyoshima C (2018) Distinct pH dependencies of Na+/K+ selectivity at the two faces of Na,K-ATPase. J Biol Chem 293:2195–2205. https://doi.org/10.1074/jbc.RA117.000700
15. Domi T, Di Leva F, Fedrizzi L, Rimessi A, Brini M (2007) Functional specificity of PMCA isoforms? Ann N Y Acad Sci 1099:237–246. https://doi.org/10.1196/annals.1387.043
16. Dyla M, Kjærgaard M, Poulsen H, Nissen P (2020) Structure and mechanism of P-type ATPase ion pumps. Annu Rev Biochem 89:583–603. https://doi.org/10.1146/annurev-biochem-010611-112801
17. de Lores Arnaiz GR, Ordieres MG (2014) Brain Na+, K+-ATPase activity in aging and disease. Int J Biomed Sci 10:85–102. https://doi.org/10.59566/ijbs.2014.10085
18. Dzneladze S, Tsakadze L, Leladze M, Nozadze E, Arutinova N, Shioshvili L, Chkadua G (2015) Comparative analysis of Mg-dependent and Mg-independent HCO3 – ATPases. J Membr Biol 248:53–58. https://doi.org/10.1007/s00232-014-9739-8
19. Fiske GH, Subbarow Y (1925) The colorimetric determination of phosphorus. J Biol Chem 66:375–400. https://doi.org/10.1016/S0021-9258(18)84756-1
20. Gerkau NJ, Lerchundi R, Nelson JSE, Lantermann M, Meyer J, Hirrlinger J, Rose CR (2019) Relation between activity-induced intracellular sodium transients and ATP dynamics in mouse hippocampal neurons. J Physiol 597:5687–5705. https://doi.org/10.1113/JP278658
21. Gu HO, Noh SW, Kim OH, Oh BC (2025) Crucial roles of calcium ATPases and phosphoinositides: insights into pathophysiology and therapeutic strategies. Mol Cells 48:100254. https://doi.org/10.1016/j.mocell.2025.100254
22. Guyenet PG, Bayliss DA (2022) Central respiratory chemoreception. Handb Clin Neurol 188:37–72. https://doi.org/10.1016/B978-0-323-91534-2.00007-2

23. Haines RW, Kirwan CJ, Prowle JR (2019) Managing chloride and bicarbonate in the prevention and treatment of acute kidney injury. Semin Nephrol 39:473–483. https://doi.org/10.1016/j.semnephrol.2019.06.007
24. Holm TH, Lykke-Hartmann K (2016) Insights into the pathology of the α3 Na(+)/K(+)-ATPase ion pump in neurological disorders; lessons from animal models. Front Physiol 7:209. https://doi.org/10.3389/fphys.2016.00209
25. Hsu KS, Liang YC, Huang CC (2000) Influence of an extracellular acidosis on excitatory synaptic transmission and long-term potentiation in the CA1 region of rat hippocampal slices. J Neurosci Res 62:403–415. https://doi.org/10.1002/1097-4547(20001101)62:3%3C403::AID-JNR11%3E3.0.CO;2-3
26. Illarionova NB, Brismar H, Aperia A, Gunnarson E (2014) Role of Na,K-ATPase α1 and α2 isoforms in the support of astrocyte glutamate uptake. PLoS ONE 9:e98469. https://doi.org/10.1371/journal.pone.0098469
27. Ivanov A, Zhao H, Modyanov NN (2000) Packing of the transmembrane helices of Na,K-ATPase: direct contact between beta-subunit and H8 segment of alpha-subunit revealed by oxidative cross-linking. Biochemistry 39:9778–9785. https://doi.org/10.1021/bi001004j
28. Johnsen LØ, Sigad A, Friis KA, Berg PM, Damkier HH (2024) NH4Cl-induced metabolic acidosis increases the abundance of HCO3 – transporters in the choroid plexus of mice. Front Physiol 15:1491793. https://doi.org/10.3389/fphys.2024.1491793
29. Kinoshita PF, Yshii LM, Vasconcelos AR, Orellana AMM, Lima LDS, Davel APC, Rossoni LV, Kawamoto EM, Scavone C (2014) Signaling function of Na,K-ATPase induced by ouabain against LPS as an inflammation model in hippocampus. J Neuroinflammation 11:218. https://doi.org/10.1186/s12974-014-0218-z
30. Kometiani Z (2007) Kinetic analysis of multi-sited enzyme systems. Pub House Sakartvelos Matsne, Tbilisi, Georgia. https://doi.org/10.52340/9789994066308t
31. Koshoridze N, Menabde K, Kuchukashvili Z (2012) Investigation of the Mg-HCO3–-ATPase activity of thyroid tissue cells under various pathologies. Scand J Clin Lab Invest 72:363–368. https://doi.org/10.3109/00365513.2012.675442
32. Kraut JA, Kurtz I (2015) Treatment of acute non-anion gap metabolic acidosis. Clin Kidney J 8:93–99. https://doi.org/10.1093/ckj/sfu126
33. Kwon TH, Fulton C, Wang W et al (2002) Chronic metabolic acidosis upregulates rat kidney Na-HCO3 – cotransporters NBCn1 and NBC3 but not NBC1. Am J Physiol Ren Physiol 282:F341–F351. https://doi.org/10.1152/ajprenal.00104.2001
34. Lardner AL, O'Donovan DJ (1997) The effect of ammonium chloride on hepatic and renal metabolism in the rat. Kidney Blood Press Res 20:57–61. https://doi.org/10.1159/000174112
35. Larsen BR, Stoica A, MacAulay N (2016) Managing brain extracellular K(+) during neuronal activity: the physiological role of the Na(+)/K(+)-ATPase subunit isoforms. Front Physiol 7:141. https://doi.org/10.3389/fphys.2016.00141

36. Lina BA, Kuijpers MH (2004) Toxicity and carcinogenicity of acidogenic or alkalogenic diets in rats; effects of feeding NH4Cl, KHCO3 or KCl. Food Chem Toxicol 42:135–153. https://doi.org/10.1016/j.fct.2003.08.011
37. Menzikov SA, Zaichenko DM, Moskovtsev AA, Morozov SG, Kubatiev AA (2021) Ectopic GABAA receptor β3 subunit determines Cl–/HCO3–-ATPase and chloride transport in HEK 293FT cells. FEBS J 288:699–712. https://doi.org/10.1111/febs.15359
38. Menzikov SA, Zaichenko DM, Moskovtsev AA, Morozov SG, Kubatiev AA (2022) Physiological role of ATPase for GABAA receptor resensitization. Int J Mol Sci 23:5320. https://doi.org/10.3390/ijms23105320
39. Menzikov SA, Zaichenko DM, Moskovtsev AA, Morozov SG, Kubatiev AA (2023) Zinc inhibits the GABAAR/ATPase during postnatal rat development: the role of cysteine residue. Int J Mol Sci 24:2764. https://doi.org/10.3390/ijms24032764
40. Meyer DJ, Bijlani S, de Sautu M, Spontarelli K, Young VC, Gatto C, Artigas P (2020) FXYD protein isoforms differentially modulate human Na/K pump function. J Gen Physiol 152:e202012660. https://doi.org/10.1085/jgp.202012660
41. National Research Council (2011) Guide for the care and use of laboratory animals, 8th edn. National Academies, Washington, DC
42. Nielsen HN, Holm R, Sweazey R, Andersen JP, Artigas P, Vilsen B (2024) Na+,K+-ATPase with disrupted Na+ binding sites I and III binds Na+ with increased affinity at site II and undergoes Na+-activated phosphorylation with ATP. Biomolecules 14:135. https://doi.org/10.3390/biom14010135
43. Nozadze E, Arutinova N, Tsakadze L, Shioshvili L, Leladze M, Dzneladze S, Chkadua G (2015) Molecular mechanism of Mg-ATPase activity. J Membr Biol 248:295–300. https://doi.org/10.1007/s00232-014-9769-2
44. Nowik M, Kampik NB, Mihailova M, Eladari D, Wagner CA (2010) Induction of metabolic acidosis with ammonium chloride (NH4Cl) in mice and rats—species differences and technical considerations. Cell Physiol Biochem 26:1059–1072. https://doi.org/10.1159/000323984
45. Palmer BF, Clegg DJ (2019) Hyperchloremic normal gap metabolic acidosis. Minerva Endocrinol 44:363–377. https://doi.org/10.23736/S0391-1977.19.03059-1
46. Peggion C, Marchionni I, Carafoli E, Brini M, Calì T (2025) Plasma membrane calcium ATPases and cerebellar pathology: what's the role in the ataxia? Biol Direct 20:109. https://doi.org/10.1186/s13062-025-00702-2
47. Percie du Sert N, Hurst V, Ahluwalia A, Alam S, Avey MT, Baker M et al (2020) The ARRIVE guidelines 2.0: updated guidelines for reporting animal research. PLoS Biol 18:e3000410. https://doi.org/10.1371/journal.pbio.3000410
48. Richards KS, Bommert K, Szabo G, Miles R (2007) Differential expression of Na+/K+-ATPase alpha-subunits in mouse hippocampal interneurones and pyramidal cells. J Physiol 585:491–505. https://doi.org/10.1113/jphysiol.2007.144733

49. Ruffin VA, Salameh AI, Boron WF, Parker MD (2014) Intracellular pH regulation by acid-base transporters in mammalian neurons. Front Physiol 5:43. https://doi.org/10.3389/fphys.2014.00043
50. Sengupta B, Stemmler M, Laughlin SB, Niven JE (2010) Action potential energy efficiency varies among neuron types in vertebrates and invertebrates. PLoS Comput Biol 6:e1000840. https://doi.org/10.1371/journal.pcbi.1000840
51. Shrivastava AN, Triller A, Melki R (2020) Cell biology and dynamics of neuronal Na+/K+-ATPase in health and diseases. Neuropharmacology 169:107461. https://doi.org/10.1016/j.neuropharm.2018.12.008
52. Slaughter BD, Urbauer RJ, Urbauer JL, Johnson CK (2007) Mechanism of calmodulin recognition of the binding domain of isoform 1b of the plasma membrane Ca(2+)-ATPase: kinetic pathway and effects of methionine oxidation. Biochemistry 46:4045–4054. https://doi.org/10.1021/bi602481u
53. Strehler EE, Caride AJ, Filoteo AG, Xiong Y, Penniston JT, Enyedi A (2007) Plasma membrane Ca2 + ATPases as dynamic regulators of cellular calcium handling. Ann N Y Acad Sci 1099:226–236. https://doi.org/10.1196/annals.1387.023
54. Zhgenti N, Bakuradze E, Bibilashvili O, Koshoridze N (2025a) The role of BDNF/PI3K/AKT/Nrf2 signaling in nicotine's protective effects against MPTP-induced Parkinson's disease. Neurosci Lett 868:138412. https://doi.org/10.1016/j.neulet.2025.138412
55. Zhgenti N, Bibilashvili O, Shengelia M, Burjanadze G, Koshoridze M, Davitashvili E, Koshoridze N (2025b) Effect of nicotine on the energy metabolism of substantia nigra cells in MPTP-induced Parkinson's disease. Iran J Basic Med Sci 28:1417–1427. https://doi.org/10.22038/ijbms.2025.84754.18338

Figures

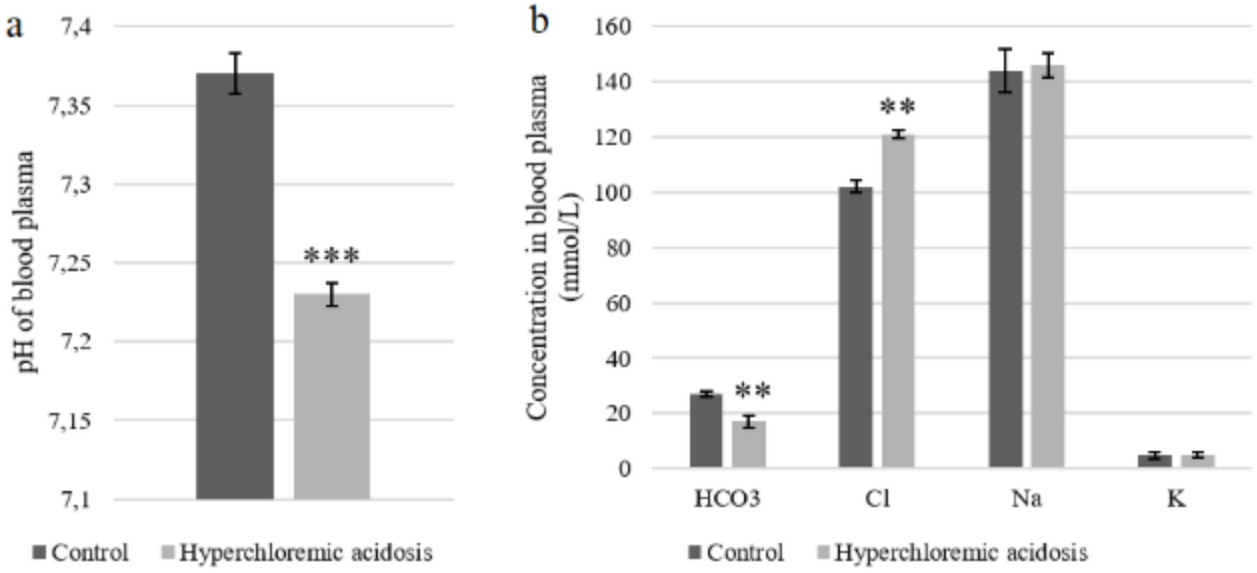


Figure 1

Effects of NH_4Cl-induced hyperchloremic acidosis on selected plasma markers. (a) Blood plasma pH; (b) Concentrations of electrolytes, including HCO_3^-, Cl^-, Na^+, and K^+, in the blood plasma of experimental animals. Data are presented as mean ± SEM (n = 15 animals per group). Statistical comparisons between groups were performed using an unpaired two-tailed Student's t-test. *p ≤ 0.05, **p ≤ 0.01, and ***p ≤ 0.001 compared with the control group (Group I)

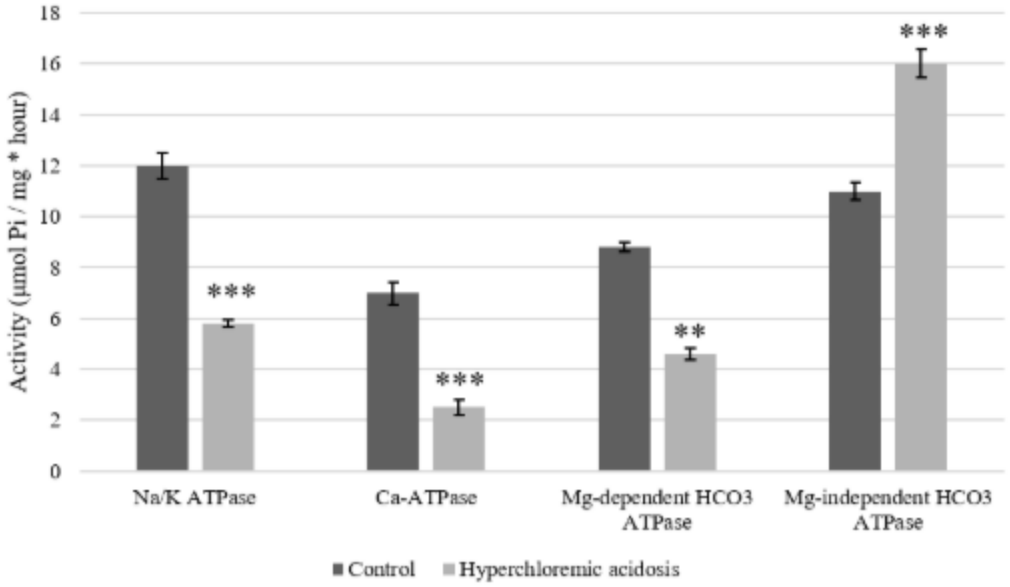


Figure 2

Effects of NH_4Cl-induced hyperchloremic acidosis on activities of Na^+/K^+, Mg-dependent Ca^{2+}, Mg-dependent HCO_3^-, and Mg-independent HCO_3^- ATPases in the hippocampus of experimental animals. Data are presented as mean ± SEM (n = 15 animals per group). Statistical comparisons between groups were performed using an unpaired two-tailed Student's t-test. *p ≤ 0.05, **p ≤ 0.01, and ***p ≤ 0.001 compared with the control group (Group I)

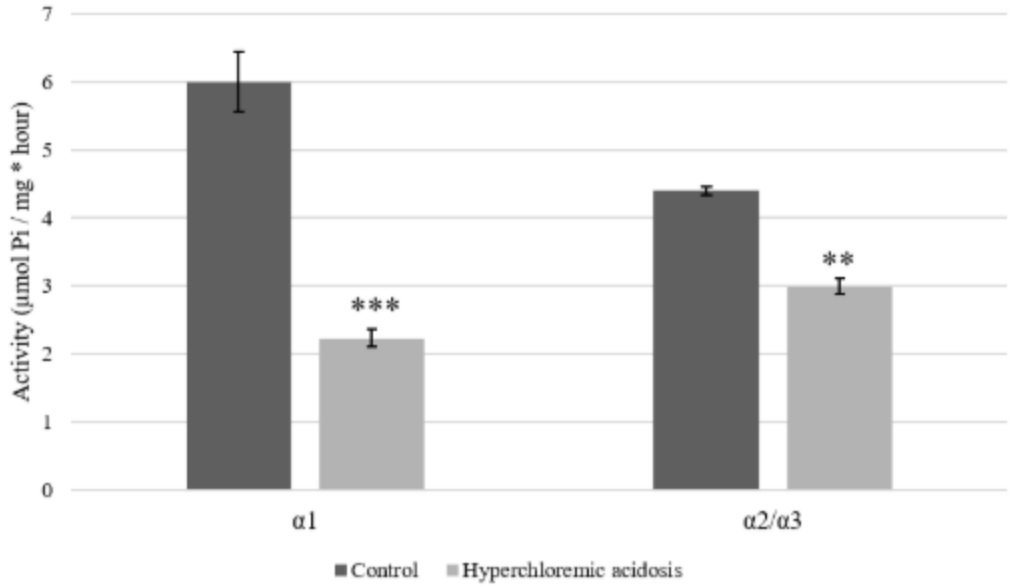


Figure 3

Effects of NH_4Cl-induced hyperchloremic acidosis on activities of Na^+/K^+ ATPase α1 and α2/3 subunits in the hippocampus of experimental animals. Data are presented as mean ± SEM (n = 15 animals per group). Statistical comparisons between groups were performed using an unpaired two-tailed Student's t-test. *p ≤ 0.05, **p ≤ 0.01, and ***p ≤ 0.001 compared with the control group (Group I). The reaction medium was [MgATP] = 1.68 mM;$[Mg_f^{2+}]$ = $[ATP_f]$ = 0.32 mM

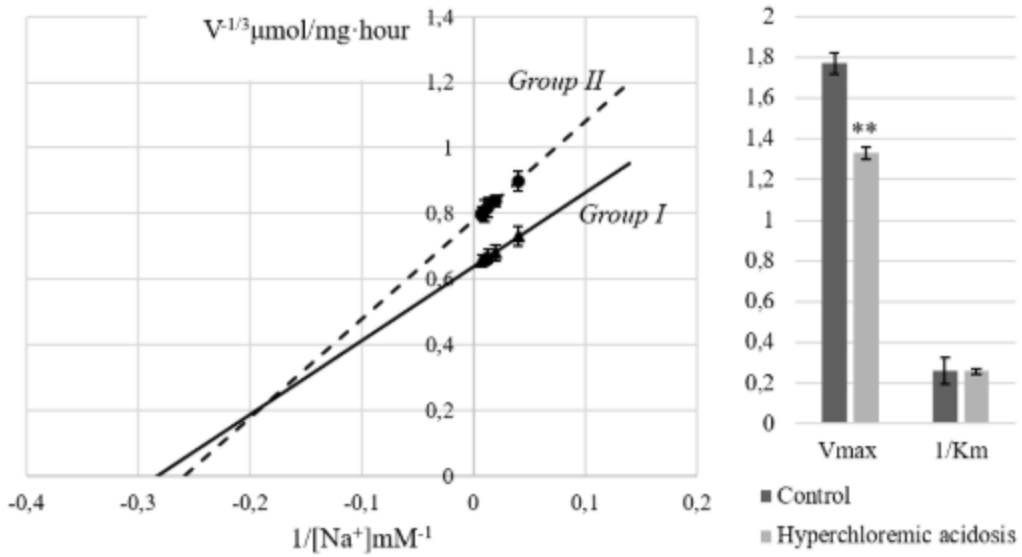


Figure 4

Effects of NH_4Cl-induced hyperchloremic acidosis on the dependence of Na/K-ATPase activity on Na^+ concentrations in the $V^{-1/3} = f(1/[Na^+])$ coordinate system. Data are presented as mean ± SEM (n = 15 animals per group). Statistical comparisons between groups were performed using an unpaired two-

tailed Student's t-test. *p ≤ 0.05, **p ≤ 0.01, and ***p ≤ 0.001 compared with the control group (Group I). The reaction medium includes [MgATP] = 1.68 mM;[Mg_f^{2+}] = [ATP_f] = 0.32 mM; [KCl]=125mM

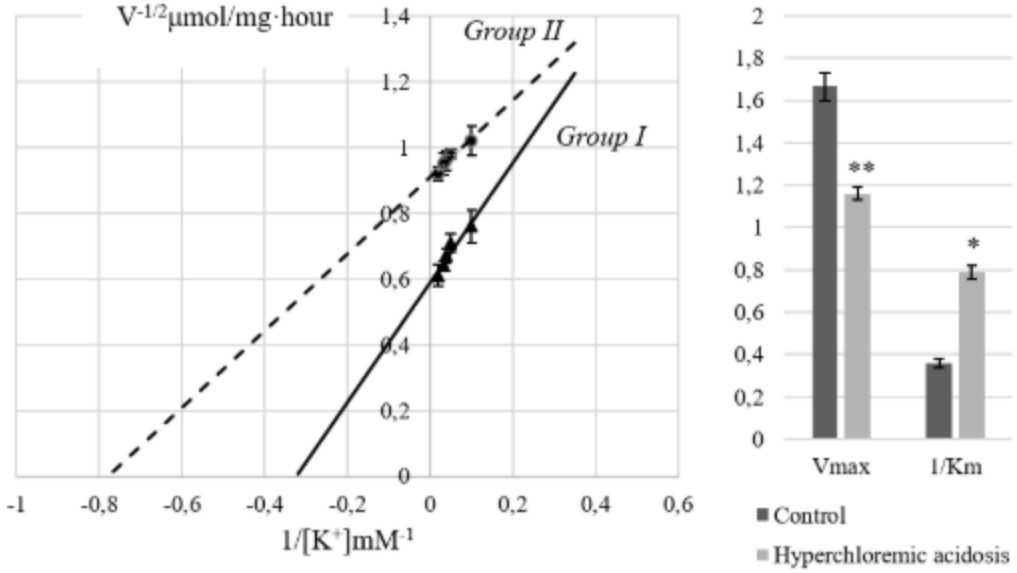


Figure 5

Effects of NH_4Cl-induced hyperchloremic acidosis on the dependence of Na/K-ATPase activity on K^+ concentrations in the $V^{-1/2}$ = f(1/[K^+]) coordinate system. Data are presented as mean ± SEM (n = 15 animals per group). Statistical comparisons between groups were performed using an unpaired two-tailed Student's t-test. *p ≤ 0.05, **p ≤ 0.01, and ***p ≤ 0.001 compared with the control group (Group I). The reaction medium includes [MgATP] = 1.68 mM;[Mg_f^{2+}] = [ATP_f] = 0.32 mM; [NaCl] = 80mM

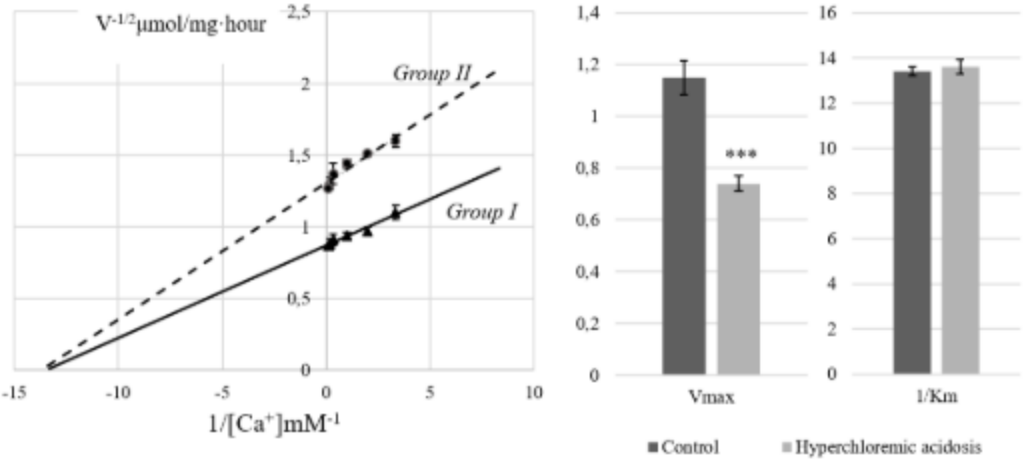


Figure 6

Effects of NH_4Cl-induced hyperchloremic acidosis on the dependence of Mg-dependent Ca^{2+}-ATPase activity on Ca^{2+} concentrations in the $V^{-1/2}$ = f(1/[Ca^+]) coordinate system. Data are presented as mean ± SEM (n = 15 animals per group). Statistical comparisons between groups were performed using an

unpaired two-tailed Student's t-test. *p ≤ 0.05, **p ≤ 0.01, and ***p ≤ 0.001 compared with the control group (Group I). The reaction medium includes [MgATP] = 1.68 mM;[Mg_f^{2+}] = [ATP_f] = 0.32 mM

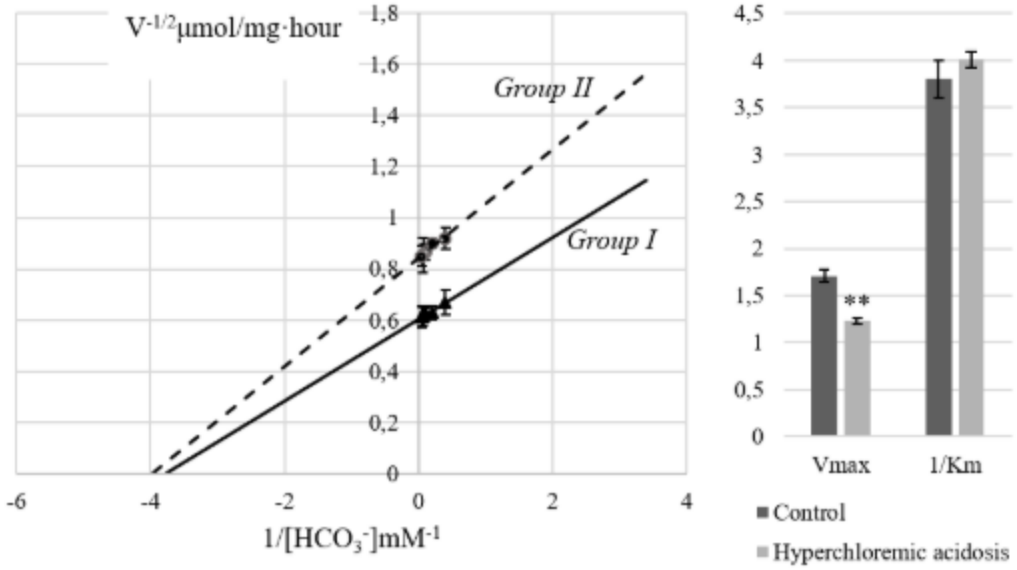


Figure 7

Effects of NH_4Cl-induced hyperchloremic acidosis on the dependence of Mg-dependent HCO_3^--ATPase activity on HCO_3^- concentrations in the $V^{-1/2} = f(1/[HCO_3^-])$ coordinate system. Data are presented as mean ± SEM (n = 15 animals per group). Statistical comparisons between groups were performed using an unpaired two-tailed Student's t-test. *p ≤ 0.05, **p ≤ 0.01, and ***p ≤ 0.001 compared with the control group (Group I). The reaction medium includes [MgATP] = 1.68 mM;[Mg_f^{2+}] = [ATP_f] = 0.32 mM

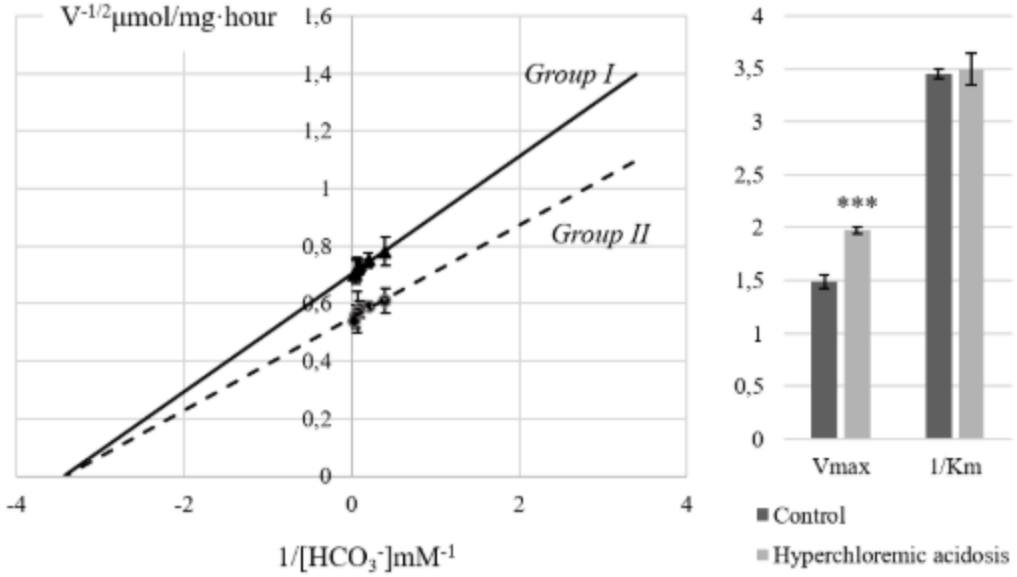


Figure 8

Effects of NH_4Cl-induced hyperchloremic acidosis on the dependence of Mg-independent HCO_3^--ATPase activity on HCO_3^- concentrations in the $V^{-1/2} = f(1/[HCO_3^-])$ coordinate system. Data are presented as mean ± SEM (n = 15 animals per group). Statistical comparisons between groups were performed using an unpaired two-tailed Student's t-test. *p ≤ 0.05, **p ≤ 0.01, and ***p ≤ 0.001 compared with the control group (Group I). The reaction medium includes $[ATP_f] = 0.32$ mM